International Journal of Theoretical Physics, Vol. 35, No. 5, 1996

Dripping Faucet

A. D'Innocenzo[1] and L. Renna[1]

Received July 6, 1995

A model for the simulation of the chaotic behavior of a leaky faucet is analyzed. It is found that the mechanism of simulating the breaking away of the drop is crucial in order to obtain the transition to chaos. Return maps and dripping spectra as functions of flow rate and critical parameters are obtained.

1. INTRODUCTION

During the last decade, following Rössler's (1977) suggestion, many authors have demonstrated experimentally that a dripping water faucet might exhibit a chaotic transition as the flow rate is varied (Marten *et al.*, 1985; Núñez Yépez *et al.*, 1989; Wu *et al.*, 1989; Wu and Schelly, 1989; Cahalan *et al.*, 1990; Dreyer and Hickey, 1991). As far as we know, mathematical models that simulate carefully this behavior have not been reported in the literature. However, several years ago, Martien *et al.* (1985) were able to simulate, by using a model of a simple one-dimensional nonlinear oscillator, some of the simpler behavior of the leaky faucet, with good qualitative agreement. These authors did not make a systematical exhaustive exploration of the dependence of the model on the parameters and claimed to obtain return maps that only in a qualitative sense, and in limited regions of the parameter space, are similar to those produced experimentally by the faucet. Furthermore, the mechanism by which the initial conditions for the drop formation were restored was not sufficiently explained. More recently, Bernhardt (1991) described a simple electronic circuit that reproduces the type of aperiodic behavior that may be found in many physical systems, such as dripping faucets, magnetospheric substorms, etc. In this paper it is demonstrated that the only nonlinearity required to yield chaos in relaxation oscillator

[1] Departimento di Fisica dell'Università, 73100 Lecce, Italy, and INFN Sezione di Lecce, Lecce, Italy.

0020-7748/96/0500-0941$09.50/0

systems is a sudden change in behavior when a threshold is reached. Bernhardt's result seems to suggest that the mechanism of formation of the drop at the threshold is crucial in order to yield chaos in mathematical models of a dripping faucet. In order to clarify this point, we have considered the model proposed in Martien *et al.* (1985) and we analyzed the effects introduced by different mechanisms of release of the drop at threshold. The amount of water which is released into the falling drop can depend on several physical quantities at the threshold, such as the speed, the mass, or the momentum of the forming drop, the time of formation of the drop, etc. Moreover, as the drop leaves the faucet, it creates oscillations in the residue (which set the initial conditions for the following drop), affecting the time of release of the next drop, so that the successive drops are causally related. This correlation between successive drops can be built up into a mathematical model in several ways: one can, for example, set the initial conditions for the following drop at the nozzle, or simulate a sudden (nonzero) reduction of the residue position. Finally, a change of the threshold can lead to further significant modifications in the results of the model.

In this paper we analyze only some of the various modalities and shapes of the formation of a drop. Our aim is to investigate a path that should lead to the establishment of the deterministic equations describing the system. In doing this we limit ourselves mainly to the study of the dependence of the model on the *parameters of the threshold*: we think in fact that, owing to the large variety of the parameters and the richness of the chaotic patterns that can be obtained, the theoretical model can be improved by exploring mostly the mechanism of threshold that, in a certain sense, is with less evidence connected to the physical constraints of the process. We believe that an investigation of the influence of the *critical* parameters of the model and the structure of the drop formation can furnish suggestions for the establishment of the mathematical equations describing the formation and successive breaking of the drops.

In Section 2, the mathematical model is explained and in Section 3 bifurcation and return map drawings obtained with fixed values of critical parameters and initial conditions are shown. In Section 4, a larger variation of parameters is performed and effects of surface tension and temperature are analyzed. Finally, conclusions are presented in Section 5.

2. MATHEMATICAL MODEL

We start from the simple mechanical model for the dripping faucet proposed in Martien *et al.* (1985). This model consists of a mass M which grows linearly with time, pulling on a spring with stretch constant k. The spring produces a linear restoring force equal to $-kx$, where x is the position

of the center of mass of the forming drop and the spring constant k represents surface tension. The damping of the residual oscillations is included in the friction force $-bv$, where $v = dx/dt$ is the speed of the center of mass of the forming drop. This unidimensional mass on a spring may be described by the equation

$$\frac{d(Mv)}{dt} = Mg - kx - bv \tag{1}$$

where g is gravitational acceleration and the mass of the drop grows at a constant rate R,

$$\frac{dM}{dt} = R \tag{2}$$

When the downward displacement of the water reaches a critical value x_c, the mass is suddenly reduced by ΔM and the position of the remaining mass oscillates according to (1) and grows according to (2). The drop mass ΔM is taken proportional to the speed dx/dt of the mass at the critical distance x_c.

There is, in this model, a certain arbitrariness in the choice of the values of the parameters, and so far an exhaustive exploration of the behavior of equation (1) in terms of these parameters has not been given. However, one cannot ignore the physics, and we believe it to be convenient to take an initial set of the parameters which is close to the physical ones. Two more aspects of the problem seem interesting: the way by means of which (a) the mass of the breaking-off drop is defined and (b) the position and speed of the successive drop in formation are related to the variables M and v at x_c.

The drop mass ΔM can be produced in several ways; we have analyzed the following:

$$\text{(i)} \quad \Delta M = \alpha M_c v_c \tag{3}$$

$$\text{(ii)} \quad \Delta M = \alpha v_c \qquad \text{(Martien } et\ al.\text{, 1985)}$$

where v_c and M_c are the speed and the mass at the threshold and α is a parameter of proportionality to be suitably adjusted. The behavior of the solutions of equations (1) and (2) depends on at least four independent parameters g, k, b, and R. In addition to these parameters we have considered, within the mechanisms of drop formation shown in relations (3), two additional parameters: the coefficient of proportionality α and the critical distance x_c. In the following we will show that the values of the last two parameters are crucial in order to obtain transition to chaos. In doing this we will maintain constant, almost everywhere, all other parameters (except, eventually, R).

As regards the relation with the initial conditions for the residue mass $m = M_c - \Delta M$, when a drop falls, one can attempt to place the residue at

the nozzle, putting $x_0 = 0$, with the speed $v_0 = v_c$, of the previous drop at the threshold. Instead, we have considered two different model systems of the breaking drop at the critical point x_c:

(a) A spherical drop and a residue point mass (*one-sphere*).

(b) Two spherical drops, one falling off, the other forming a residue for the successive drop (*two-sphere*).

Figure 1a shows the system of point mass and sphere; the system center of mass is at x_c; the initial position for the residue mass is given by

$$x_0 = x_c - r\frac{\Delta M}{M_c} \tag{4}$$

where $r = (3\Delta M/4\pi\rho)^{1/3}$ and ρ is the liquid density. Figure 1b shows the two-sphere model; with the center of mass at x_c we obtain for the position of the residue the relation

$$x_0 = x_c - (r_1 + r_2)\frac{\Delta M}{M_c} \tag{5}$$

where $r_{1,2} = (3\Delta M_{1,2}/4\pi\rho)^{1/3}$ and $M_1 = \Delta M$, $M_2 \equiv m = M_c - \Delta M$.

By setting in both models $v_0 = v_c$ the total momentum **P** is unaffected by the breaking. In the following section, by choosing values of the parameters g, k, and b near the physical ones, corresponding to a standard experimental apparatus, we give an exhaustive study of the two modalities of the drop formation (3) with the previously suggested breaking shape of Fig. 1a. Work is in progress in order to extend the analysis to the breaking shape of Fig. 1b (D'Innocenzo and Renna, n.d.); a preliminary result is given in the following.

3. NUMERICAL SIMULATIONS

We have set the initial values of the parameters with reference to the physical properties of the drops.

As the surface tension represents a force per length, we have, for a *water* drop, a value of k roughly equal to 500 dynes/cm, while the friction force depends on the liquid viscosity η and on the eyedropper characteristics.

A preliminary test was performed, on the basis of which we have set throughout $k = 475$ dynes/cm, $b = 1$ sec^{-1}, $m = 0.01$ g, and $v_0 = 0.10$ cm/sec. This choice is justified by the necessity of limiting the number of variables of the model: however, one must keep in mind that there exist other values of these parameters for which a sensible variation of the solutions can be obtained. For example, intermittencies with period doubling of a period-

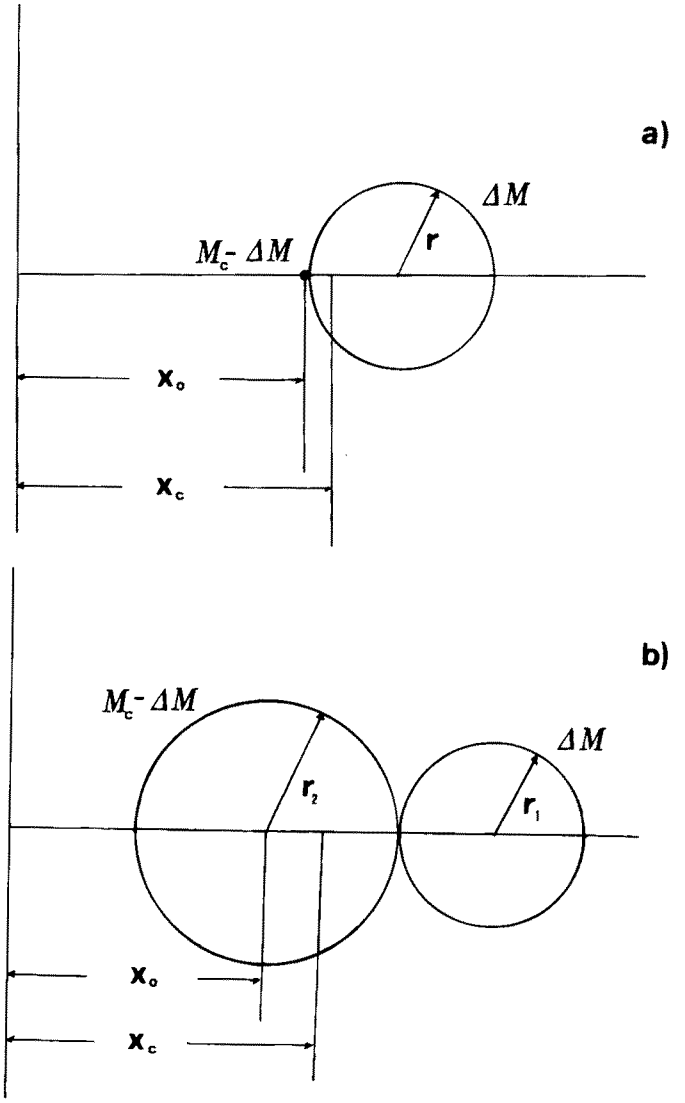

Fig. 1. Mechanism of drop breaking at the threshold: (a) one-sphere and (b) two-sphere models.

3 attractor or chaotic patterns are obtained for $m = 0.10$ g. In Section 4 a larger variation of parameter values is carried out.

Substituting the solution

$$M(t) = m + Rt \tag{6}$$

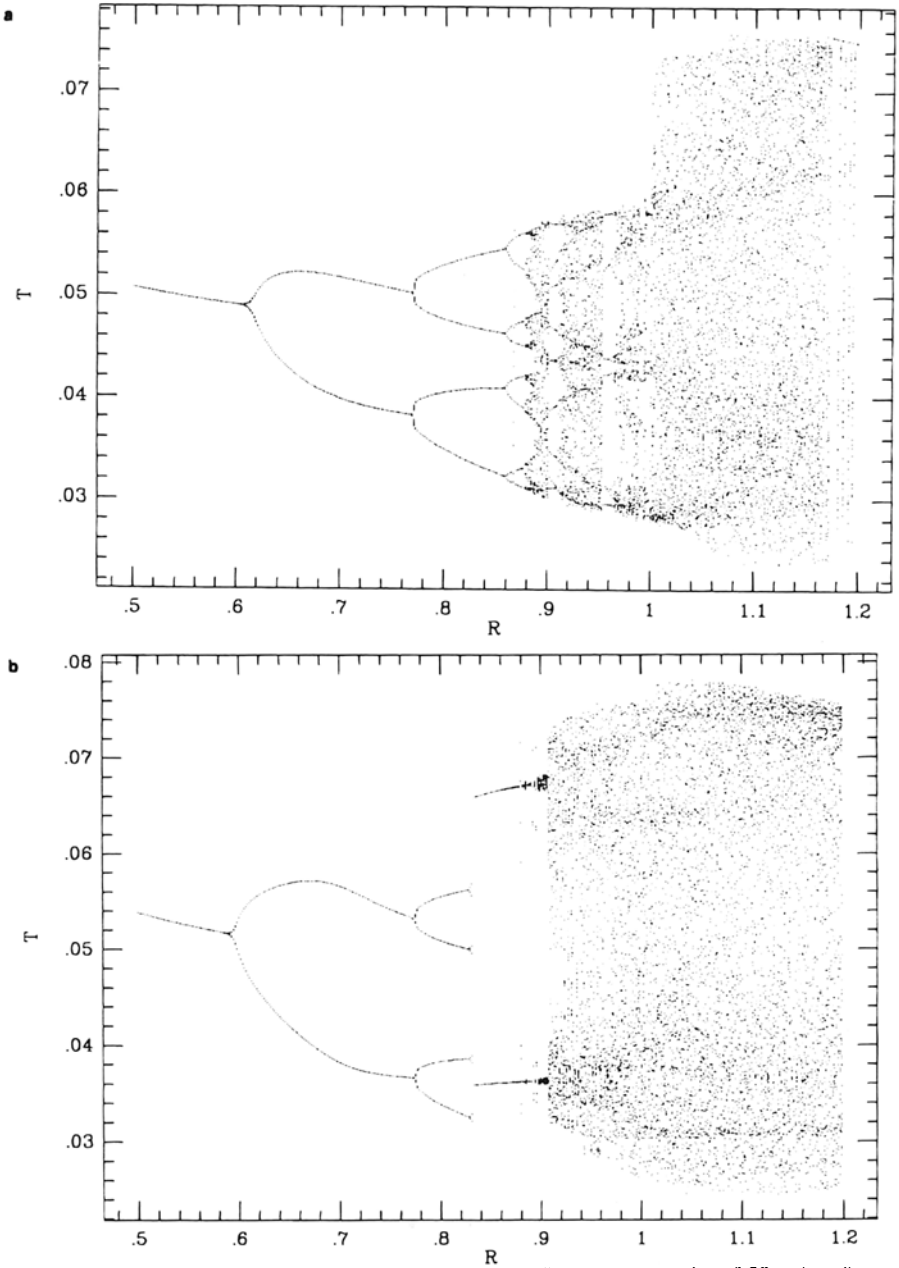

Fig. 2. Drip spectra: (a) $\Delta M \propto M_c \nu_c$; (b) $\Delta M \propto \nu_c$. The spectra consist of 50 points for each R value. The values of the other parameters are given in the text.

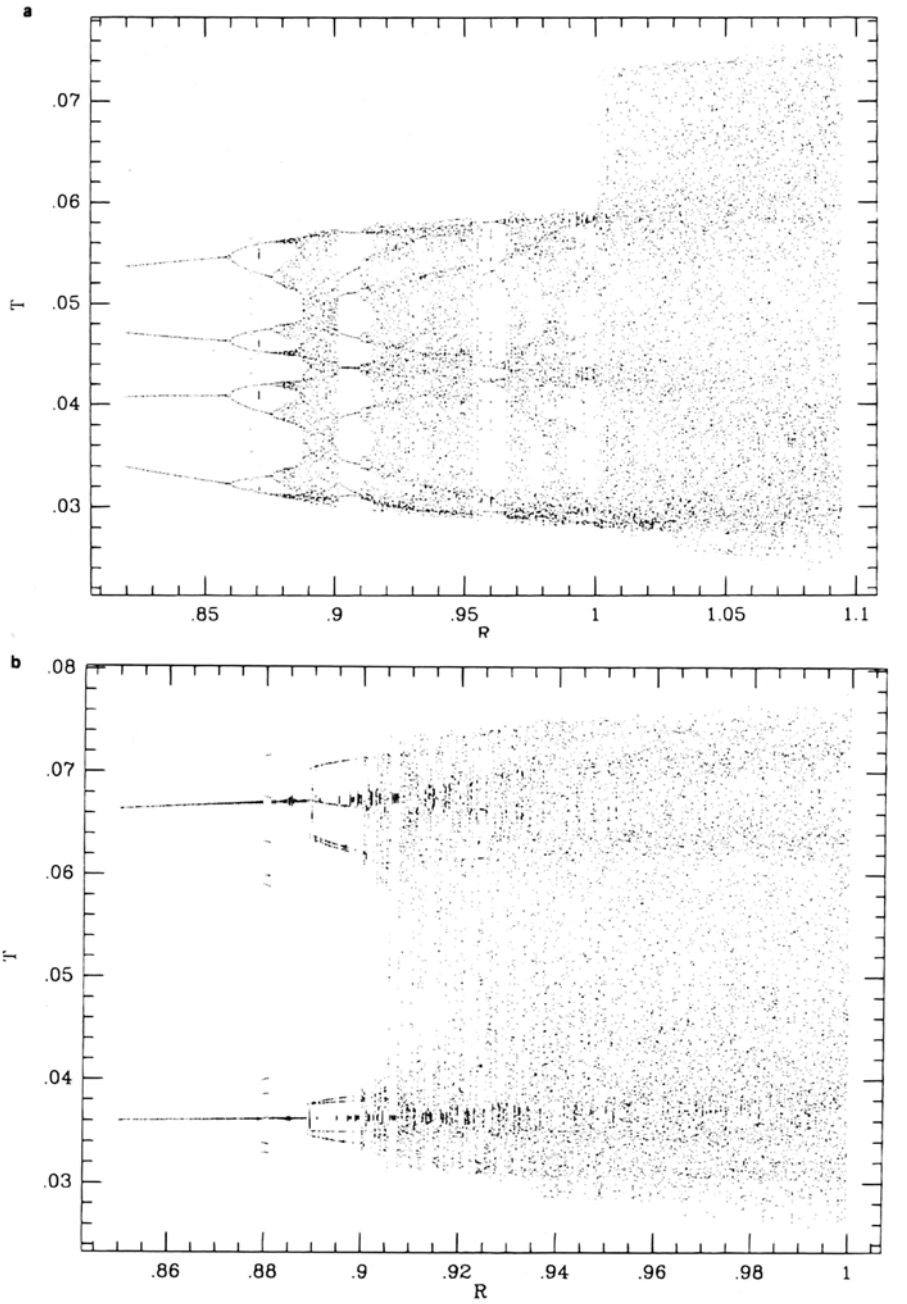

Fig. 3. Enlargement of spectra of Fig. 2.

Table I. Parameters Kept Fixed

m	v_0	k	g	b	x_c
0.01 g	0.1 cm/sec	475 dynes/cm	980 cm/sec^2	1 g/sec	0.19 cm

of equation (2) into equation (1) and introducing the speed $v = dx/dt$, we transform these equations into the equivalent system

$$\frac{dx}{dt} = v \tag{7}$$

$$M\frac{dv}{dt} = Mg - kx - (R + b)v$$

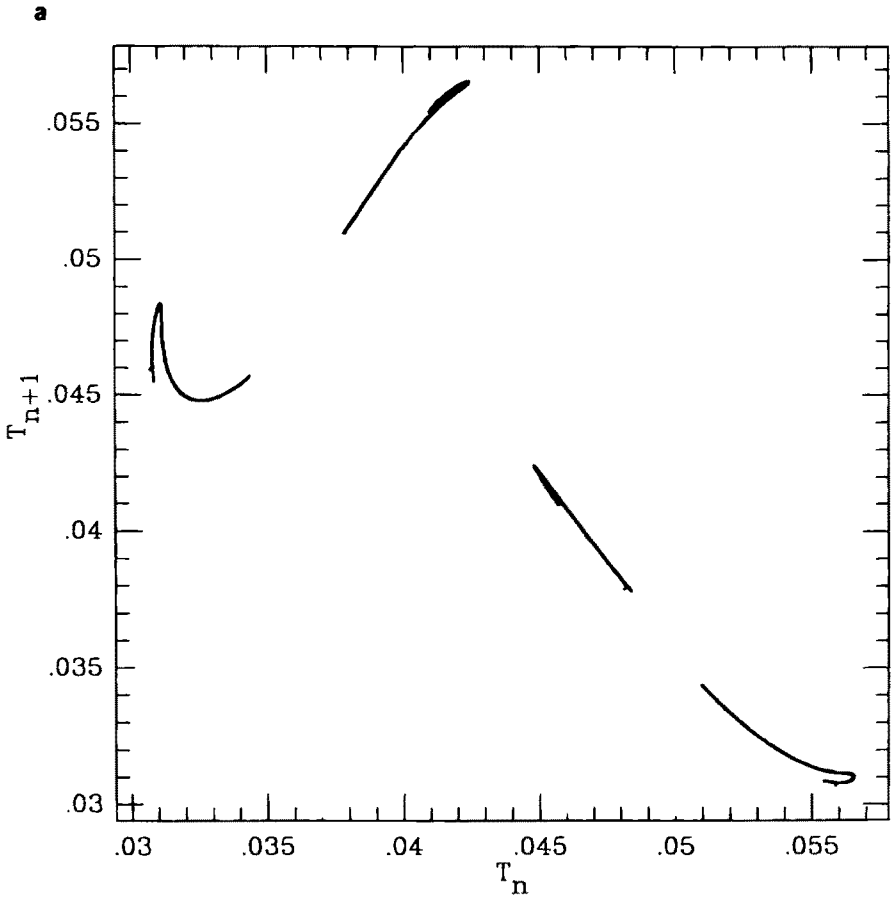

Fig. 4. Dripping patterns (T_{n+1} versus T_n) for $\Delta M \propto M_c v_c$. The ranges for ordinates and abscissae are the same (units, seconds). Flow rate (ml/sec): (a) 0.885, (b) 0.95, (c) 1.05.

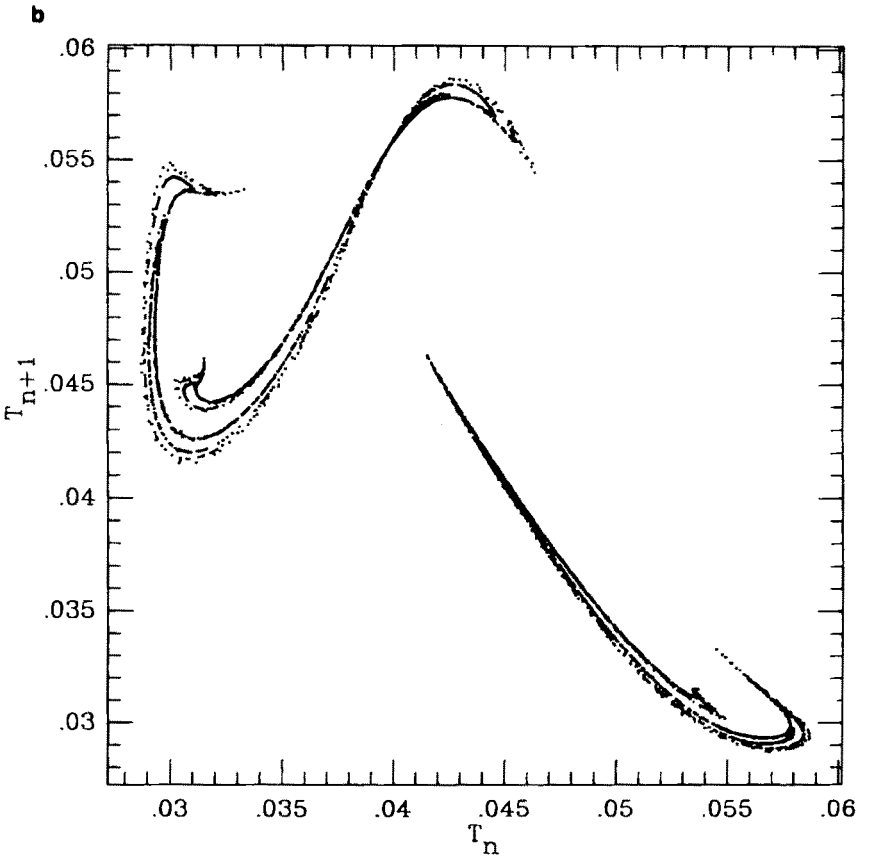

Fig. 4. Continued.

whose numerical solutions are obtained by means of a standard variable-step fourth-order Runge-Kutta method in the modification due to Gill (see Butcher, 1987). Equations (7) are integrated until x exceeds x_c: thus the integration is performed back to x_c by using the Hénon (1982) method for the numerical computation of Poincaré maps. In our calculations we have verified that in any case the fluid flow rate is always conserved.

Table I gives the values of the parameters that we have kept fixed. The experimental behavior of a dripping faucet during the transition to chaos has been examined by several authors (Martien *et al.*, 1985; Núñez Yépez *et al.*, 1989; Wu *et al.*, 1989; Wu and Schelly, 1989; Cahalan *et al.*, 1990; Dreyer and Hickey, 1991). The experiments involve measurement of time intervals between successive drips. For each constant flow rate, the data are represented in a time delay diagram (t_{n+1} versus t_n) or discrete map.

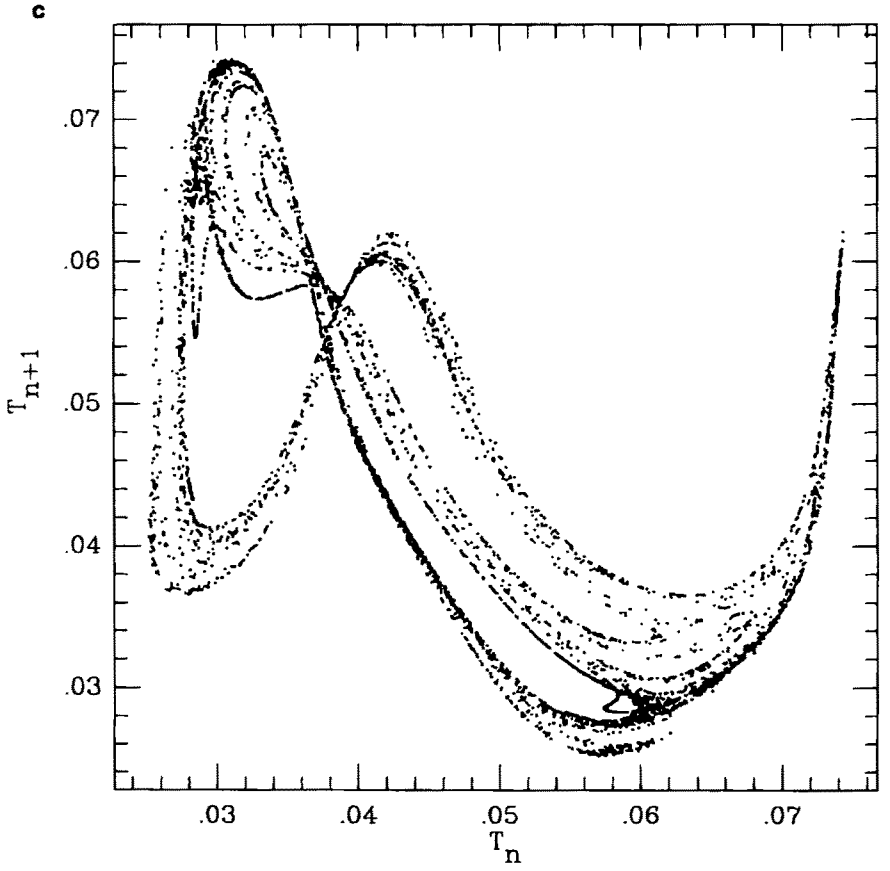

Fig. 4. Continued.

The experimental investigations can be summarized as follows. At low flow rate, dripping is found to be periodic (period-1 and period-2 attractors). As the flow rate is varied and set to increasingly larger values, a period-doubling sequence leading, above a critical flow rate, to chaos appears; the system exhibits a broad range of dynamical behavior, with many examples of strange attractors. Examples of an intermittent route to chaos, with period-3 and period-4 attractors, are also given (Dreyer and Hickey, 1991). Varying the surface tension dramatically changes the dynamics (Wu and Schelly, 1989).

As in both previous theoretical and experimental studies, we have focused our attention on the time interval t_n between successive drips. Figure 2 shows the drip spectra of water versus R, with ΔM given in Fig. 2a by formula (i) and Fig. 2b formula (ii) of (3) (the first 150 of 200 drops

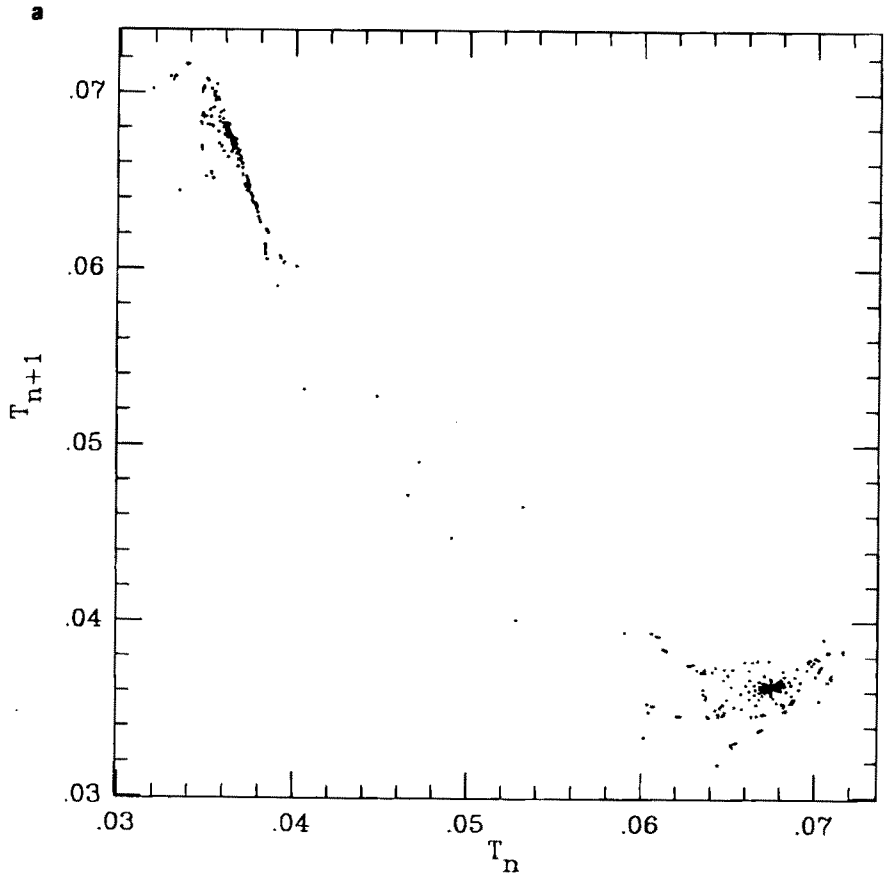

Fig. 5. Dripping time delay diagrams for $\Delta M \propto v_c$. Ranges and units as in Fig. 4. Flow rate: (a) 0.90, (b) 0.94, (c) 1.0.

are removed). These are clear diagrams of bifurcations: in Fig 2a at $R \simeq 0.61$ ml/sec there is a bifurcation from an attractor of period 1 to an attractor of period 2. As R is increased, successive bifurcations occur until strange periodic attractors appear. Analogous results are obtained in Fig 2b; up to $R \simeq 0.825$ ml/sec the behavior is the same as in Fig. 2a, then a biperiodic dripping leading to chaos appears. We have used for model (i) $\alpha = 0.25$ cm^{-1} sec, for model (ii) $\alpha = 0.025$ g cm^{-1} sec^{-1}, and $x_c = 0.19$ cm for both.

The enlargement of the spectra in Fig. 3 reveals the flow rates at which characteristic behaviors occur: for instance, in Fig. 3a transitions to different attractors are easily seen; bistability can be observed in Fig. 3b around flow rates ranging up to $\simeq$0.92 ml/sec. Figures 4 and 5 show time delay diagrams at three selected flow rates; each of these diagrams contains 5×10^3 points

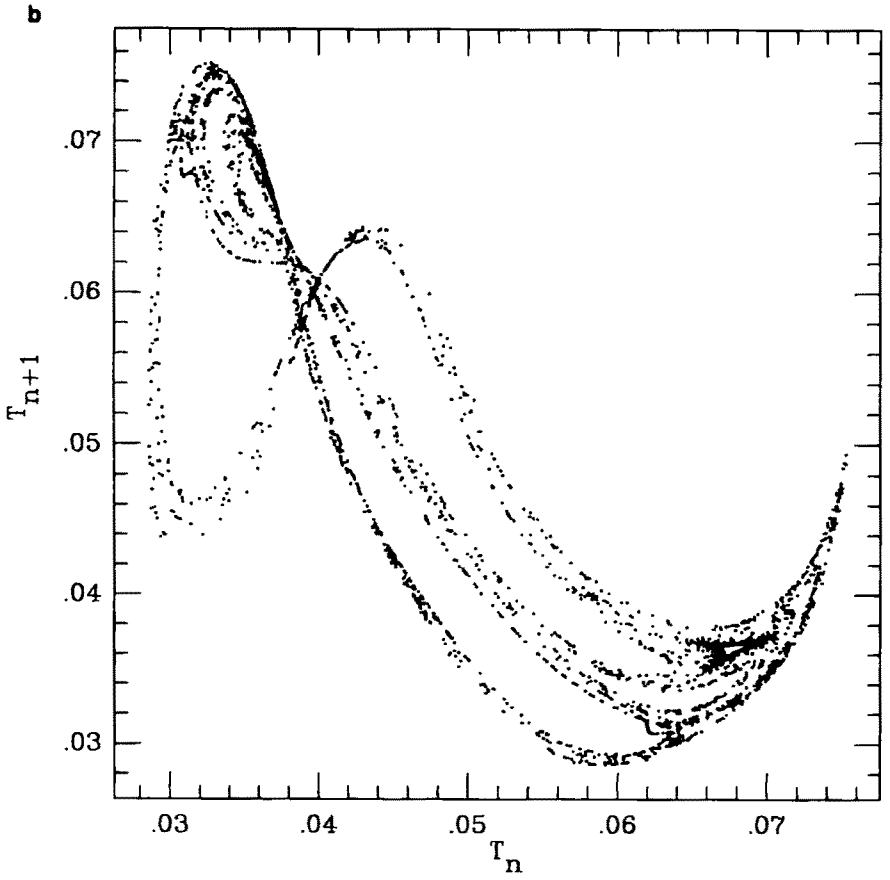

Fig. 5. Continued.

(the first 10 points are removed). It can be observed in Fig. 4 that the complexity of the attractor grows with increasing R; a sharp change occurs at $R = 1.025$ ml/sec (see also Fig. 3a). An analogous change occurs for Fig. 3b at $R = 0.93$ ml/sec. As it can be seen from Figs. 5 and 6 with ΔM proportional to the speed, the attractors seem to change from a period-2 state to a chaotic state, but the analysis of the data shows two curious aspects of the time of release. First, one can observe the resemblance of the attractors in parts (b) and (c) of Figs. 4 and 5 in spite of the difference of the flow rate spectra: this can be explained by observing that in case (a), $\alpha = 0.25$ cm^{-1} sec, while in case (b), $\alpha = 0.025$ g cm^{-1} sec; this similarity can be understood since at the threshold both calculated masses are of the order of $M_c \simeq 0.1$ g. The second aspect is evident in Fig. 6, where time series diagrams of Figs. 5a and 5b are shown: in both diagrams, after a long transitory chaotic

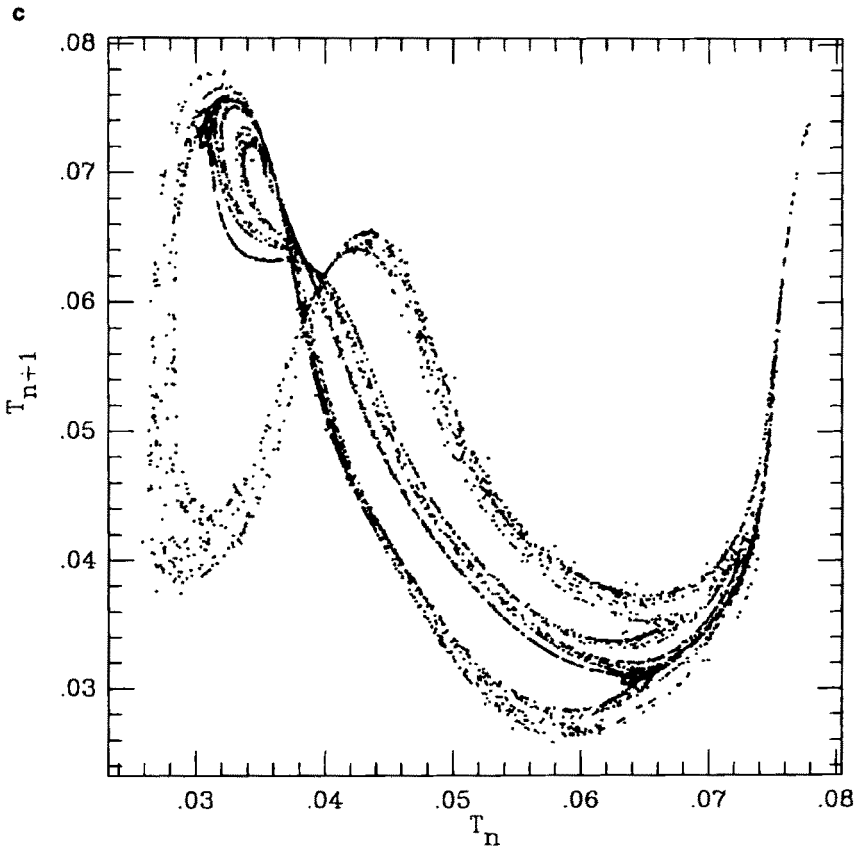

Fig. 5. Continued.

rhythm, the time intervals alternate, exhibiting biperioding dripping: this happens after 250 drops in case (a), but after 2200 drops in case (b); thus this effect is not evidenced by the dripping spectra of Figs. 2b and 3b, which contain 50 drops. This behavior appears at $R = 0.95$ ml/sec. An analogous effect happens for case (i) at $R = 0.93$ ml/sec; however, in this case a chaotic pattern transforms after 800 drips to a multiperiodic pattern. As far as we know, these phenomena are not reported in the experimental studies.

We finish this section by showing in Fig. 7 the drip spectra at $R = 0.9$ ml/sec as a function of the critical distance x_c. These diagrams are useful in that they suggest a strong dependence of the model on this parameter; the spectra calculated at different flow rates can furnish useful indications in order to obtain different forms for the chaotic attractor. Observing Fig. 7b, one can see an anomalous decrease of the dripping time intervals as the critical distance x_c grows in the case where the drop mass ΔM is taken

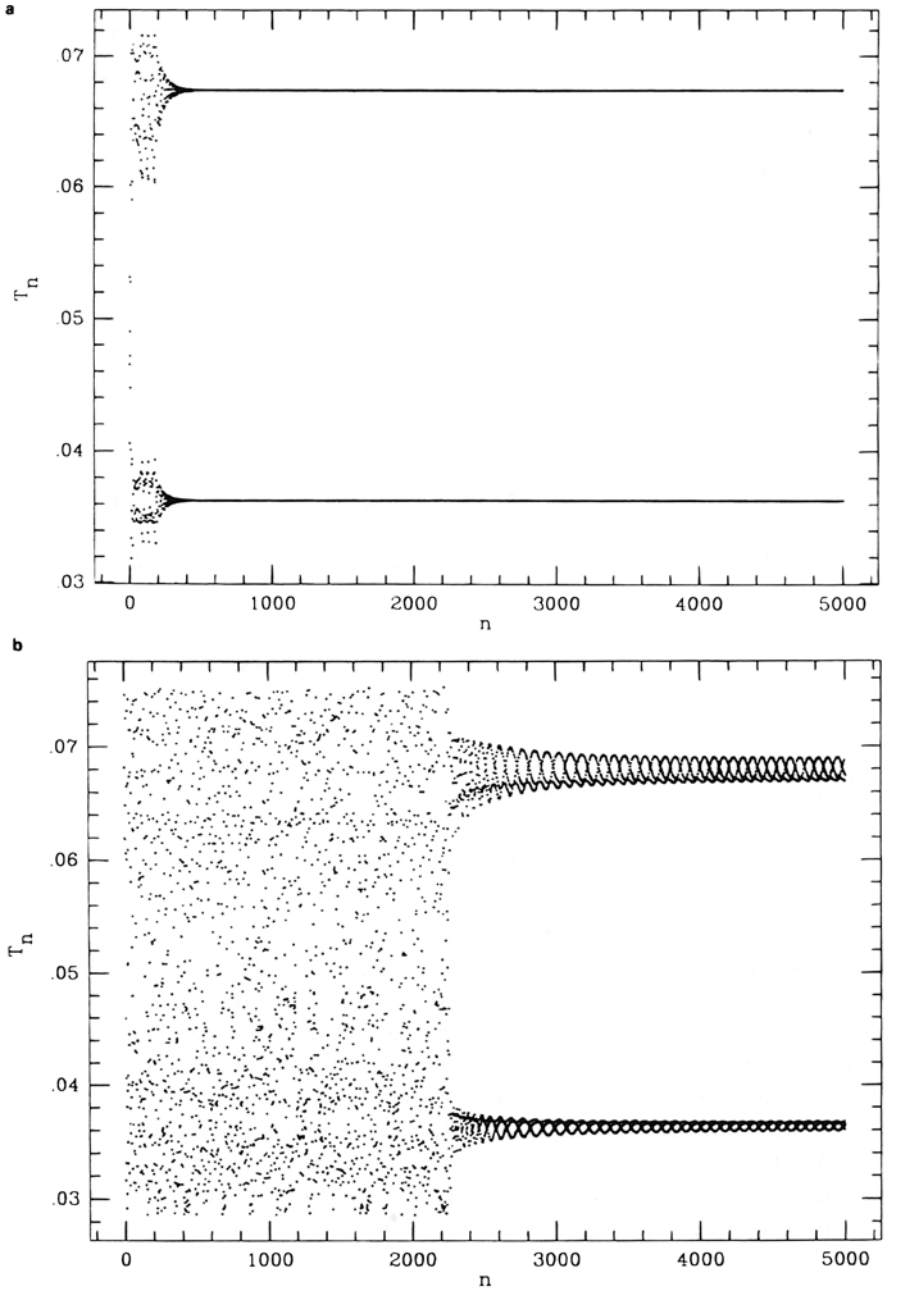

Fig. 6. Time interval versus drop number for Figs. 5a and 5b.

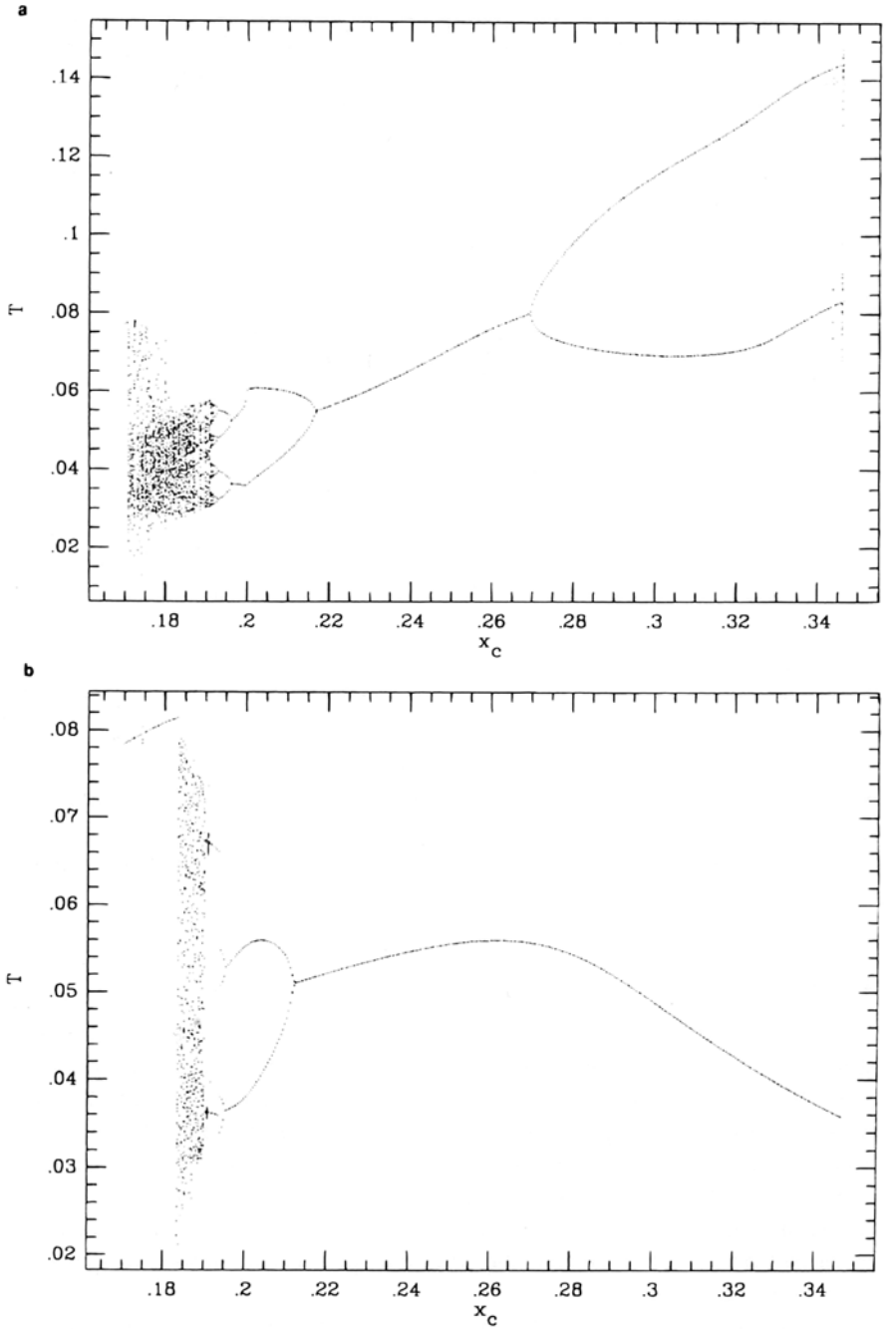

Fig. 7. Drip spectra as function of the critical distance x_c (units, cm) at $R = 0.90$ ml/sec: (a) $\Delta M \propto M_c v_c$, (b) $\Delta M \propto v_c$.

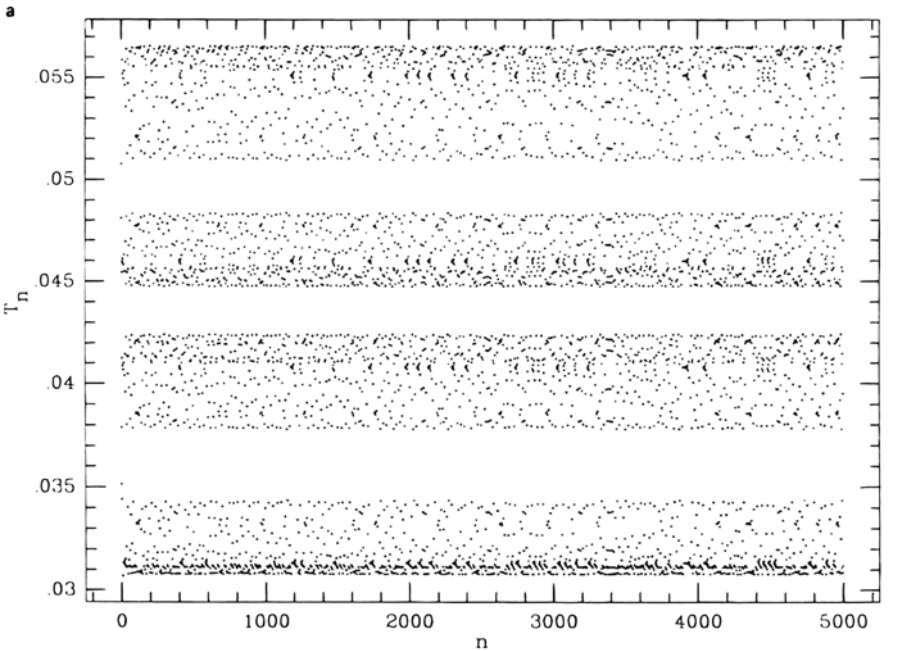

Fig. 8. Time series diagram for the drop interval of Fig. 4a. (b–e): Time delay diagrams of the four attractors of the time series in (a). (f) Sixty successive drop intervals connected with straight lines for enhanced visual effect.

proportional to the drop speed v. This argument seems to privilege the model (i) over (ii) of relation (3).

Moreover, all these results suggest that a correct model of a dripping faucet must contain a certain dependence among α, x_c, and R.

4. ATTRACTORS

Figure 8 shows the case illustrated in Fig. 4a in greater detail: the time series diagrams show four patterns that evolve in the chaotic attractors of Figs. 4b and 4c. In the time delay diagrams of Figs 8b–8e the four attractors of the time series of Fig. 8a are shown separately. The shape of Fig. 8d can be obtained from the shape of Fig. 8c by a double reflection about the time axes. In Fig. 8f 60 successive drop intervals from the middle of the time series of Fig. 8a are connected with straight lines for enhanced visual effect in order to see more clearly the alternate periodic behavior of the drop time intervals.

Some interesting maps are obtained upon varying both x_c and α. Figure 9 shows some attractors for case (i) of (3); these attractors are very similar

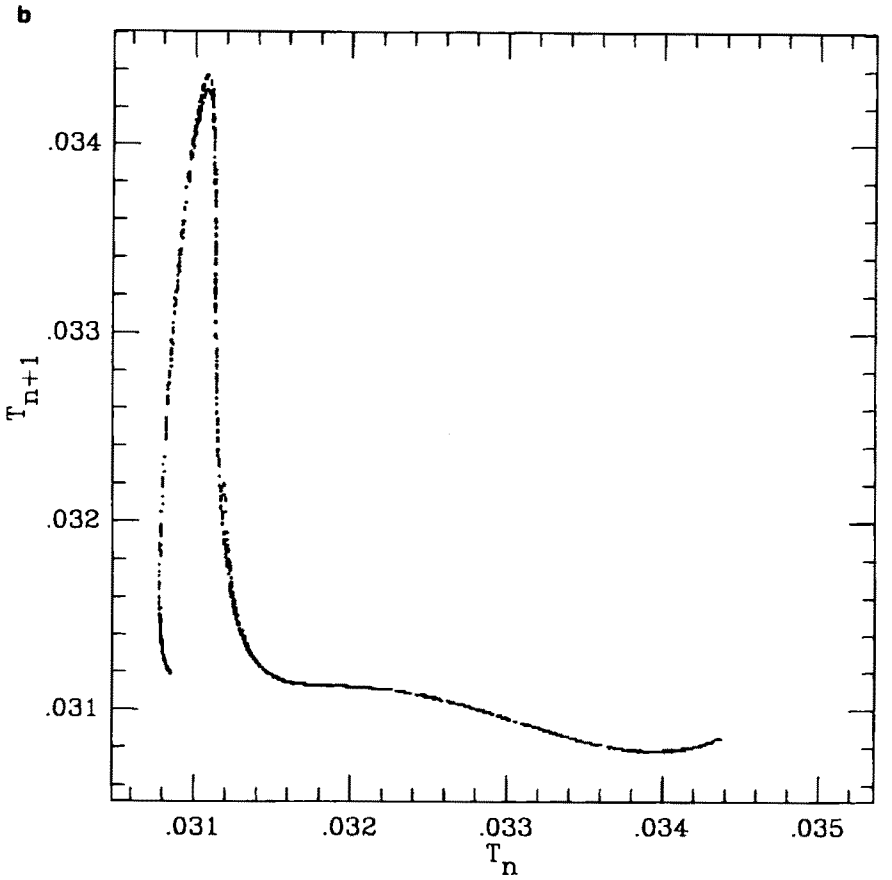

Fig. 8. Continued.

to experimental attractors. The dependence on these parameters is evidenced on comparing the map of Fig. 9b with that of Fig. 9d, whose attractor structure is quite different.

The effect of changing the liquid surface tension has been also analyzed; results are reported in Fig. 10 for a flow rate of 0.95 ml/sec. It can be noted that the strange attractor of Fig. 4b becomes biperiodic with decreasing surface tension (k = 450 dynes/cm), while it evolves into an attractor of more complex structure for k = 500 dynes/cm.

Finally, we show some delay diagrams and the corresponding time series for the two-sphere model of Fig. 1b. In Fig. 11 an attractor-type dinosaur is obtained with drop mass $\Delta M \propto M_c v_c$, while in Fig. 12, taking $\Delta M \propto v_c$, we show a closed discrete attractor with a suggestive regularity in the time series behavior.

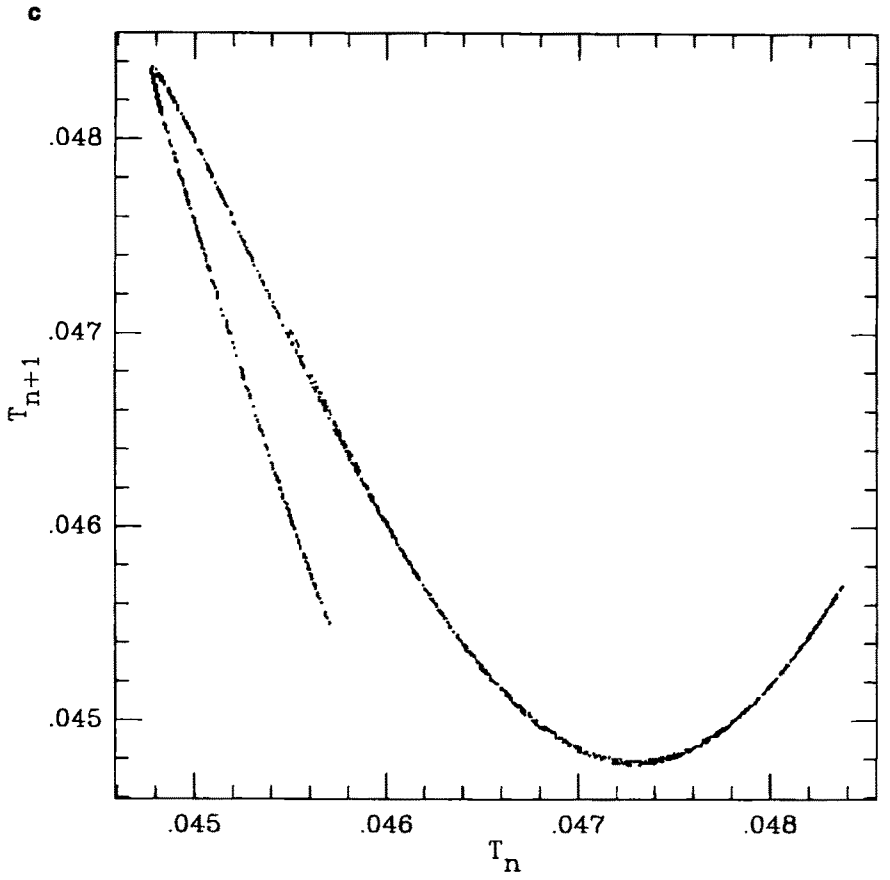

Fig. 8. Continued.

Thus with the present model several features of the dripping faucet behavior can be observed as closed-loop patterns and periodic or strange attractors.

5. CONCLUSIONS

The model of a dripping faucet we have presented in this paper reproduces many of the experimental behaviors. In addition, it contains a dynamics which reveals many interesting features. Further investigations can be performed in order to understand the nature of various attractors and the effect of those parameters which are not varied in our analysis. This mathematical model displays in fact various forms of chaos and thus lends itself well to

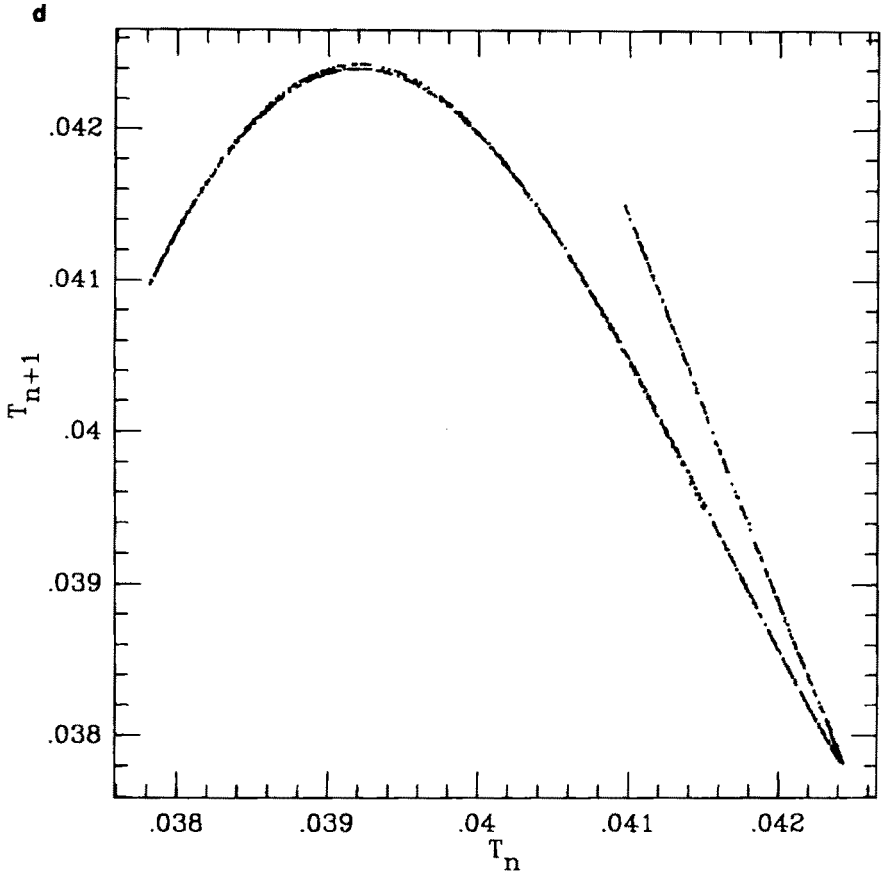

Fig. 8. Continued.

the representation of typical phenomena of nonlinear physics. The results of our work can be summarized as follows:

(i) The differential equations (1) and (2), with *one* prefixed mechanism for the release of the drop, seem to us unable to reproduce all the characteristic patterns of the dripping faucet.

(ii) The *relevant* nonlinearity required to yield chaos is given by the *sudden changes* at the threshold.

(iii) A consistent definition of *threshold* is necessary in order to give unicity to the model.

(iv) The mechanism of release of the drop with a mass proportional to momentum seems to be more realistic.

(v) *A link between the threshold parameters* is necessary in order to obtain a more complete reproduction of experimental results.

We think that further studies along the above lines can lead to a good refinement of the model.

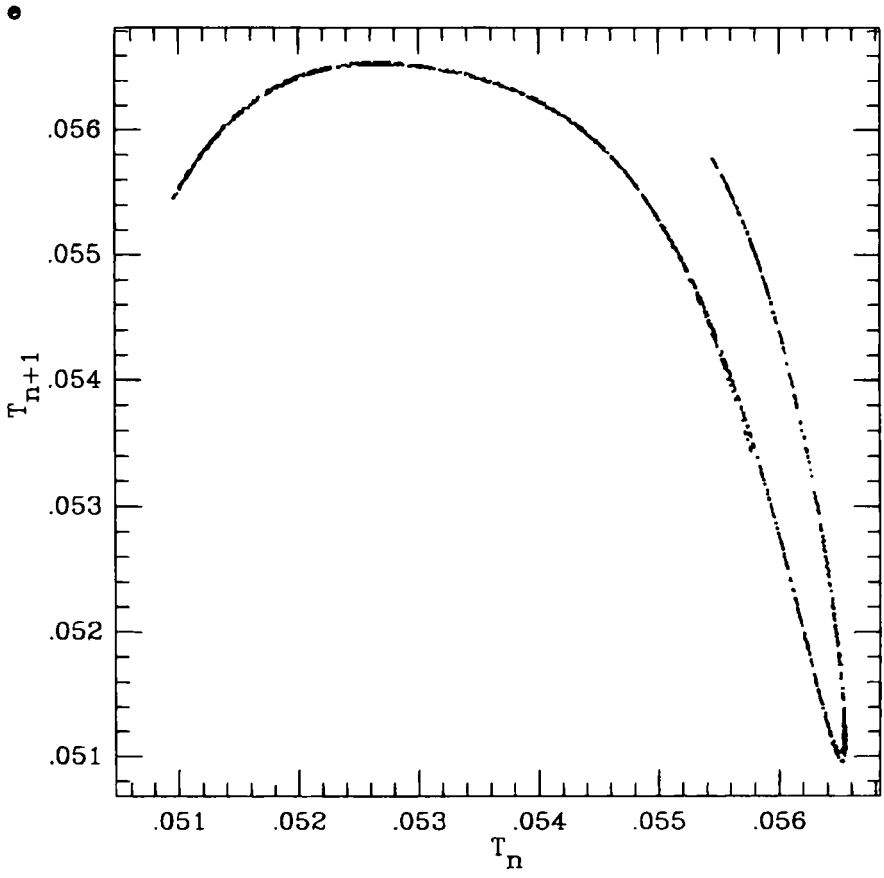

Fig. 8. Continued.

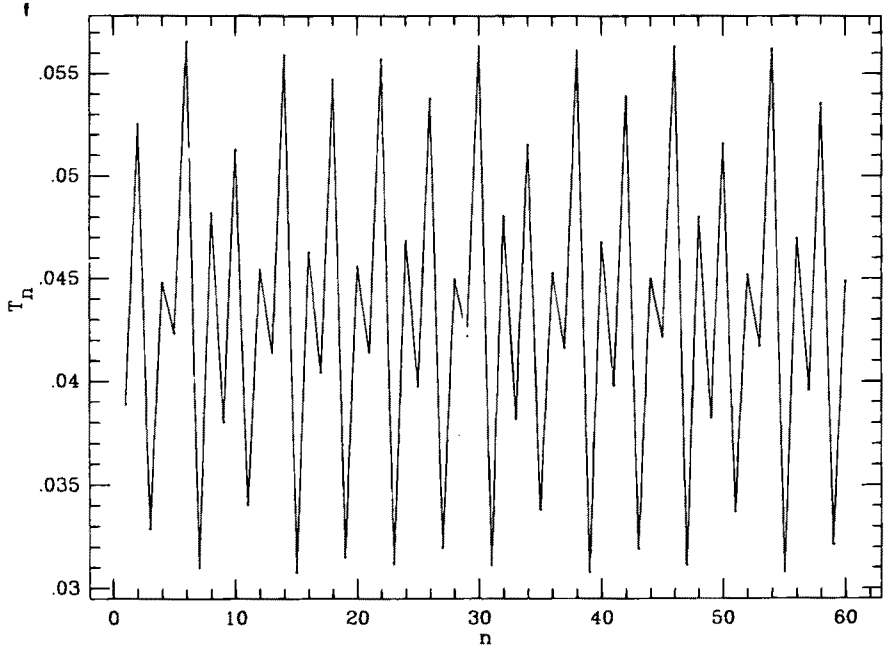

Fig. 8. Continued.

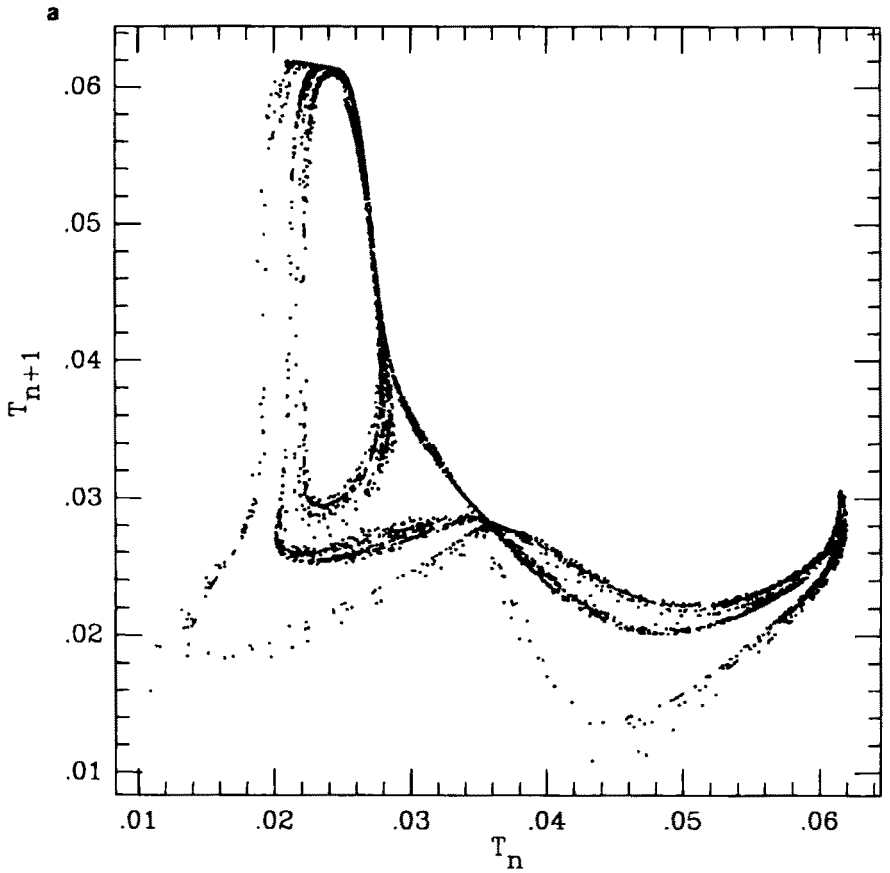

Fig. 9. Examples of strange attractors for $\Delta M \propto M_c v_c$. The values of α (units cm^{-1} sec) R (ml/sec), x_c (cm) are, respectively: (a) $\alpha = 0.2$, $R = 1.3$, $x_c = 0.15$; (b) $\alpha = 0.3$, $R = 0.4$, $x_c = 0.15$; (c) $\alpha = 0.4$, $R = 0.6$, $x_c = 0.25$; (d) $\alpha = 0.5$, $R = 0.3$, $x_c = 0.3$; (e) $\alpha = 0.6$, $R = 0.6$, $x_c = 0.25$.

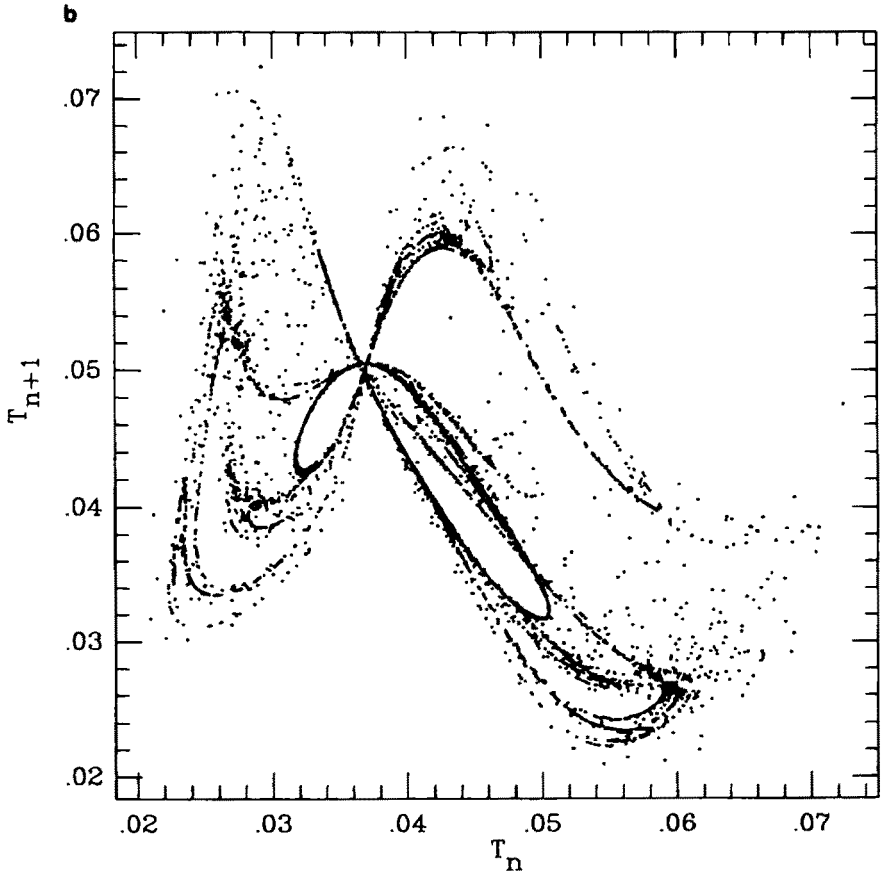

Fig. 9. Continued.

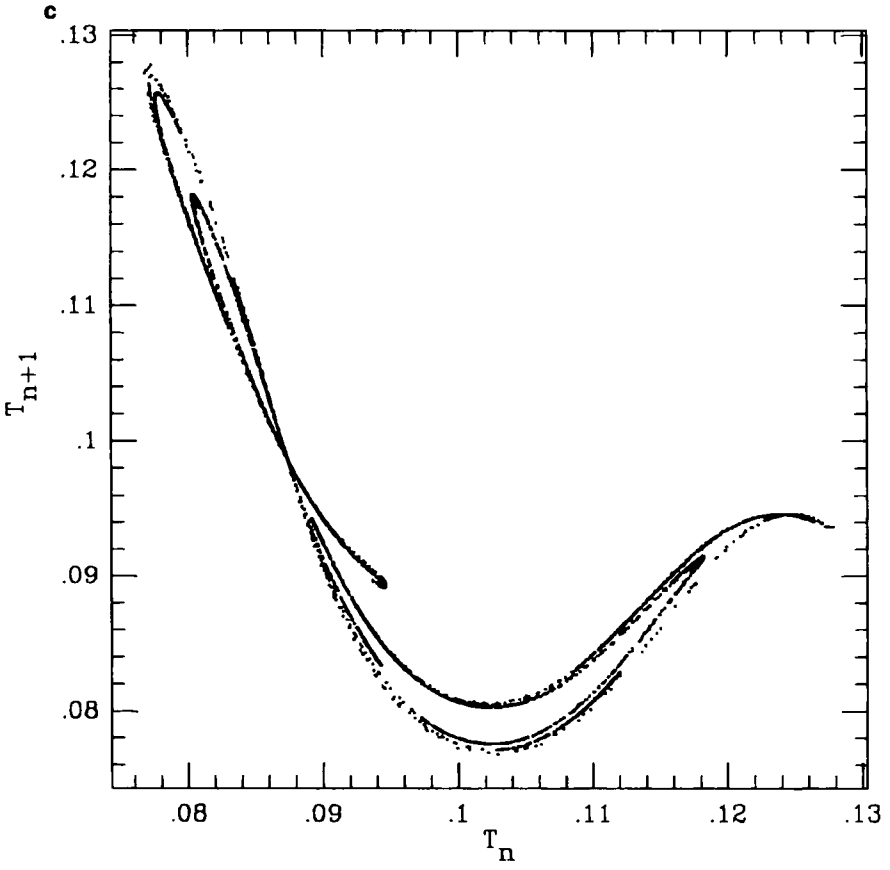

Fig. 9. Continued.

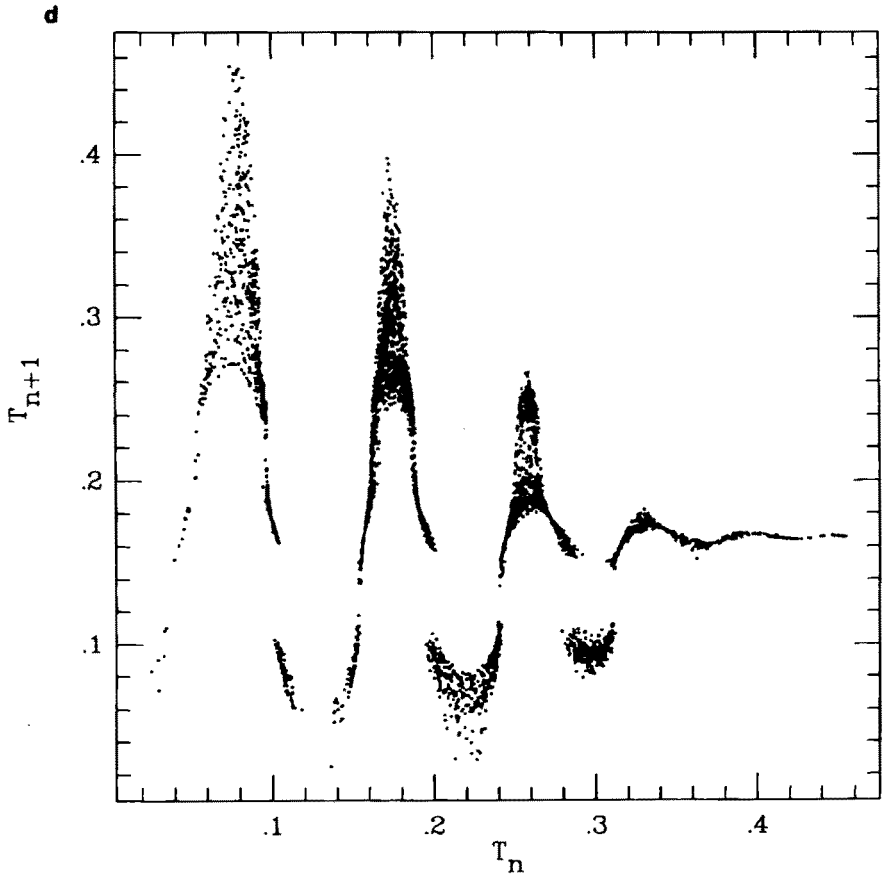

Fig. 9. Continued.

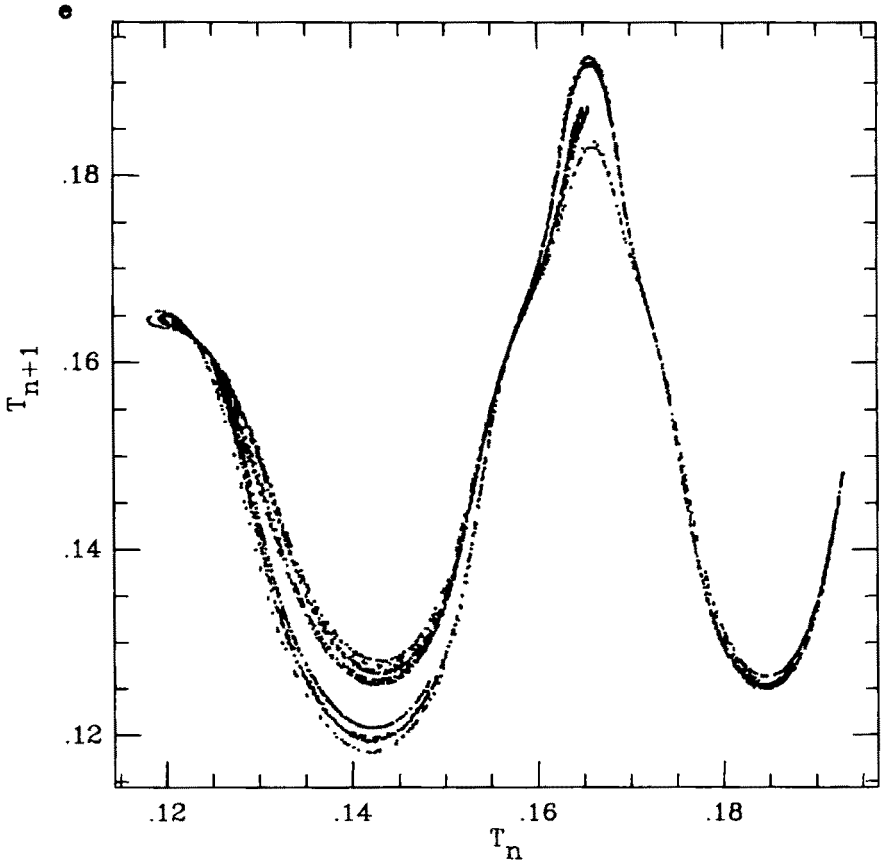

Fig. 9. Continued.

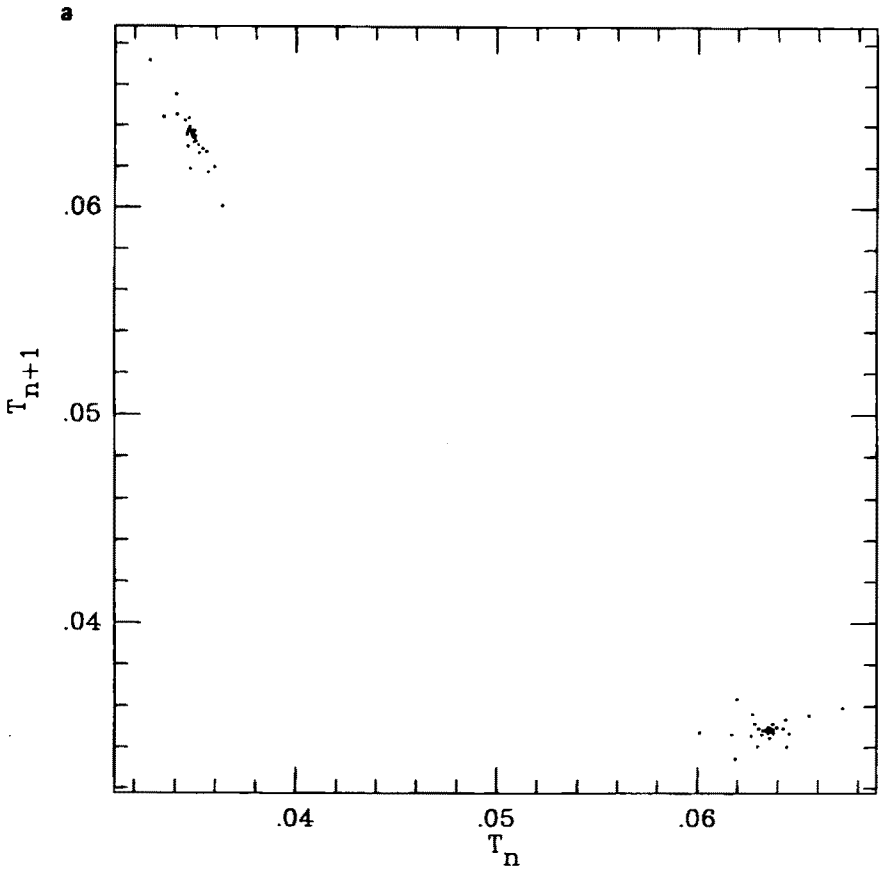

Fig. 10. Effects of changing the surface tension on the drip patterns. (a) $k = 450$ dynes/cm; (b) $k = 500$ dynes/cm. The other parameters are the same as for Fig. 4b.

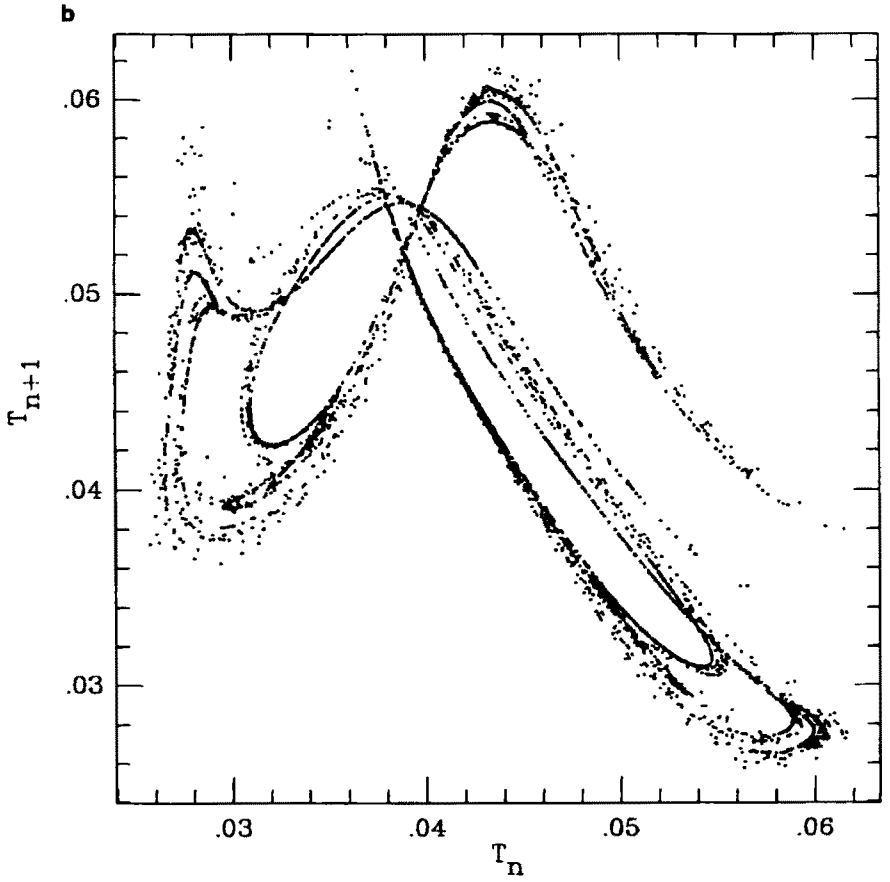

Fig. 10. Continued.

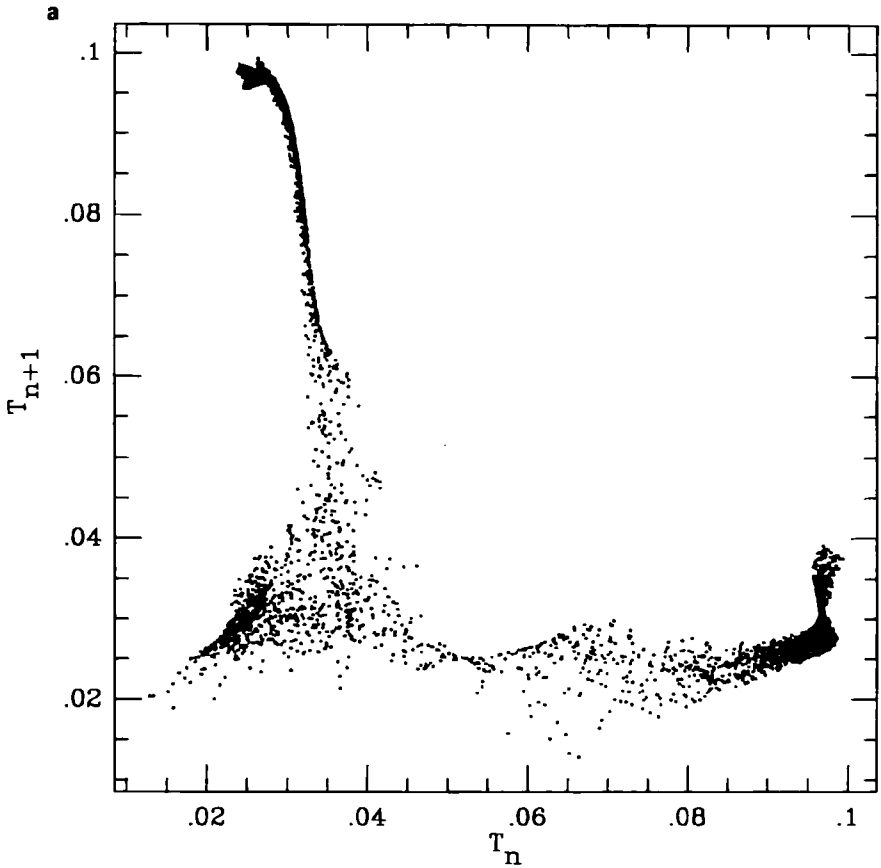

Fig. 11. (a) Discrete map and (b) time series diagram for the two-sphere model with $\Delta M \propto M_c v_c$. Values of the parameters are $\alpha = 1$, $R = 0.9$, $x_c = 0.25$. Units are as in the previous figures for the case $\Delta M \propto M_c v_c$.

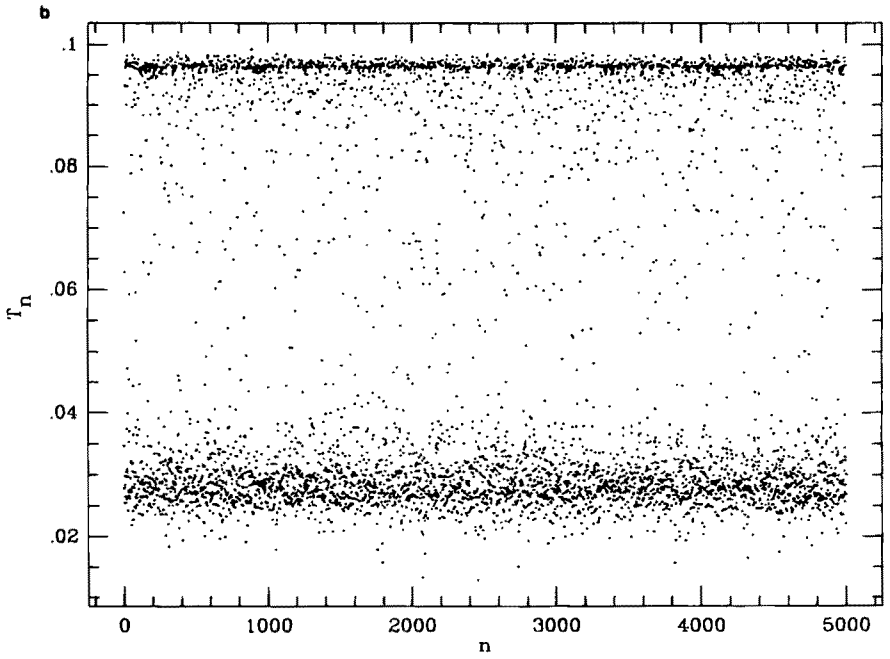

Fig. 11. Continued.

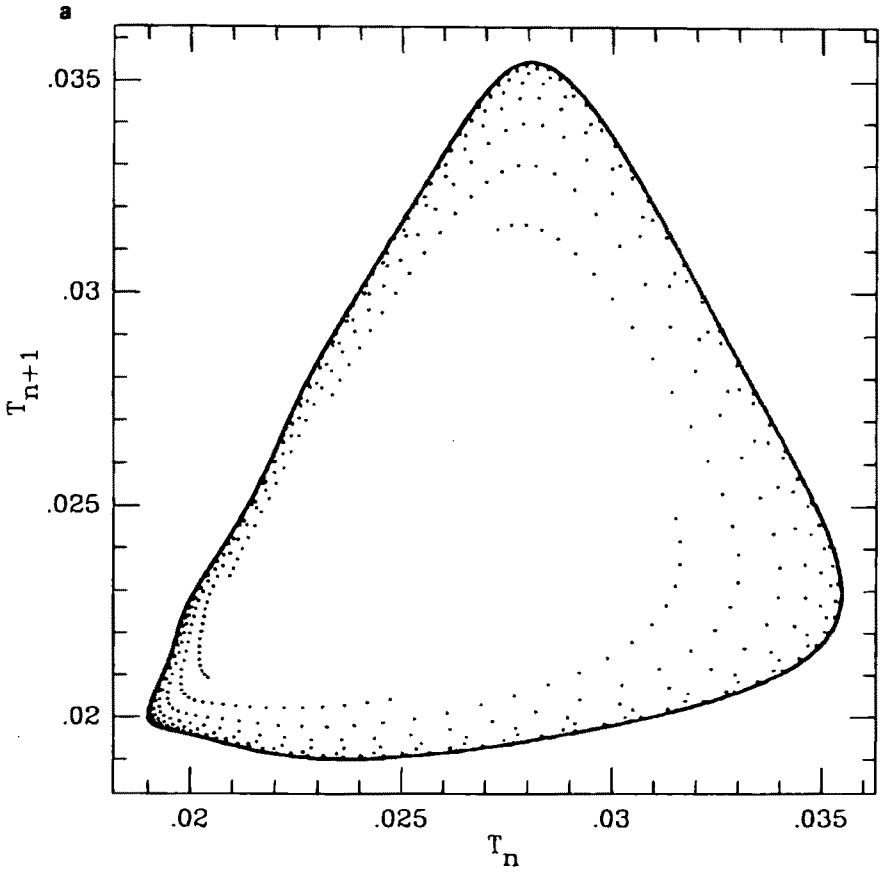

Fig. 12. (a) Discrete map and (b) time series diagram for the two-sphere model with $\Delta M \propto v_c$. Values of the parameters are $\alpha = 0.008$, $R = 0.9$, $x_c = 0.3$. Units are as in the previous figures for the case $\Delta M \propto v_c$.

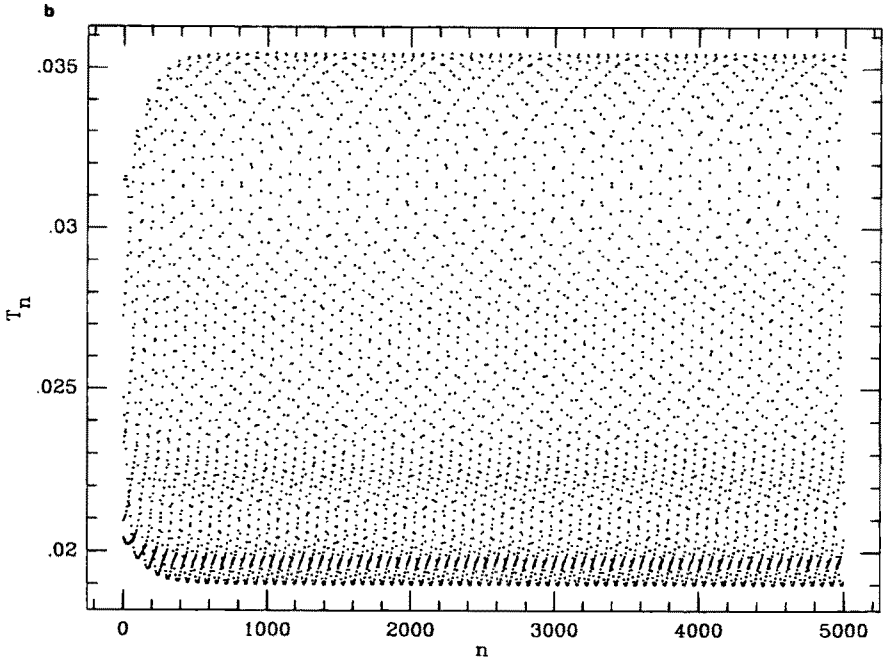

Fig. 12. Continued.

NOTE ADDED IN PROOFS

After submission of this paper for publication, the authors became acquainted with an article by J. C. Sartorelli, W. M. Gonçalves, and R. D. Pinto (Physical Review **E, 49** (1994), 3963), in which experimental evidences of sudden changes from chaotic to periodic regimes of a dripping faucet have been reported. These results are very similar to those shown in Fig. 6a and 6b of this paper and are considered by the authors as strong encouragement to continue the study of these phenomena.

REFERENCES

Bernhardt, P. A. (1991). *Physica D*, **52**, 489.

Butcher, J. C. (1987). *The Numerical Analysis of Ordinary Differential Equations*, Wiley, New York, p. 181.

Cahalan, R. F., Leidecker, H., and Calahan, G. D. (1990). *Computers in Physics*, **4**, 368.

D'Innocenzo, A., and Renna, L. (n.d.). In preparation.

Dreyer, K., and Hickey, F. R. (1991). *American Journal of Physics*, **59**, 619.

Hénon, M. (1982). *Physica*, **5D**, 412.
Martien, P., Pope, S. C., Scott, P. L., and Shaw, R. S. (1985). *Physics Letters*, **110A**, 399.
Núñez Yépez, H. N., Salas Brito, A. L., Vargas, C. A., and Vicente, L. A. (1989). *European Journal of Physics*, **10**, 99.
Rössler, O. E. (1977). In *Synergetics, A Workshop*, H. Haken, ed., Springer, Berlin, p. 174.
Wu, X., and Schelly, Z. A. (1989). *Physica D*, **40**, 433.
Wu, X., Tekle, E., and Schelly, Z. A. (1989). *Review of Scientific Instruments*, **60**, 3779.